Chapter 3

Detection of Amazon Forest Degradation Caused by Land Use Changes

Paul Arellano, Kevin Tansey and Heiko Balzter

Additional information is available at the end of the chapter

http://dx.doi.org/10.5772/65493

Abstract

Field and satellite optical methods for estimation of chlorophyll content were applied in three study sites of the Ecuadorian Amazon rainforest. Those sites represent a wide range of land use disturbance in secondary and pristine lowland rainforest. The first field method is based on transmittance from the SPAD-502 chlorophyll meter index, the second field method is based on reflectance measurements collected by a spectroradiometer, and the third method estimates chlorophyll content from the PROSPECT radiative transfer model. For the first method, seven models that account for a wide range of vegetation species showed similar average leaf chlorophyll contents until 80 units of SPAD-502. An average of the results of these models was computed and used as ground truth from where a generalized second-order polynomial model was created. For the second method, five chlorophyll indices based on reflectance measurements provided similar chlorophyll content estimations for all SPAD range (15–95 units). The third method estimates chlorophyll content based on the inversion process of the PROSPECT model. The satellite methods estimate vegetation indices sensitive to chlorophyll content from space. All methods have shown to be an alternative approach to detect forest degradation at local and regional levels caused by forest disturbances and land use changes.

Keywords: tropical forest, chlorophyll content, remote sensing, land use, forest degradation, photosynthesis

1. Introduction

The Amazon rainforest holds half of the tropical forested area of the world [1] and accounts for 30% of global biomass productivity [2] and 25% of global biodiversity [3]. Evaporation and condensation in tropical forests play a pivotal role in the regional and global atmospheric circulation [4], and the rivers' system produces about 20% of the world's fresh water discharge [5]. Photosynthesis and respiration process are more than twice the carbon of the annual rate of anthropogenic fossil fuel emissions [6]. Tropical forests store large amounts of carbon in high diversity ecosystems and play an important role in the global carbon cycle due to its net primary productivity (NPP). According to the estimates of Ref. [7], Amazon forests contain 70–80 billion metric tons (Pg or 10^{15} g) of carbon in plant biomass and assimilate 4–6 Pg of carbon each year in NPP. Despite its importance, a better understanding is needed of the interactions between the tropical forest and the global processes, such as climate change. During the last decades, the Amazon forest has been threatened by deforestation, selective logging, hunting, fire, and global and regional climate changes [4, 5].

Tropical forest deforestation and degradation have raised international concerns since they contribute approximately 20% to the global greenhouse gases (GHGs) emissions [8]. Reducing emissions from deforestation and forest degradation (REDD) is a United Nations Framework Convention on Climate Change (UNFCCC) initiative that developed a financial framework and mechanisms to reduce forest losses and the associated GHGs emissions aiming to prevent further deforestation and consequently mitigate climate change.

Deforestation is defined as the "permanent" conversion of a forest type to another land cover. "Forest degradation" is a reduction in biomass density within a forest cover. The relative contribution of deforestation and degradation to the net emissions of carbon is not readily distinguished [9]. Research has aimed to quantify global deforestation from satellite and census data, but there is an ongoing debate on the uncertainties of the estimates [10]. On the other hand, forest degradation has been more difficult to measure with remote sensing and there are no estimates for the entire tropics [9]. Therefore, accurate estimations of photosynthetic activity of forested areas are needed to quantify forest degradation and evaluate environmental services provided by flora in the tropical forest.

Photosynthesis is probably the most important biochemical process on earth. It allows plants to absorb certain wavelengths of the incoming radiation from the sun and transform its energy into organic compounds. Photosynthetically active radiation (PAR) is the amount of sunlight in the 400–700 nm wavelength range that is available for photosynthesis. Its agents are the photosynthetic pigments in the chloroplasts of which chlorophyll is the most important.

The leaf chlorophyll content is closely related to the plant's health and physiology. This characteristic has been considered to assess vegetation stress in agricultural areas and forest plantations [11–14], but studies of chlorophyll content in tropical rainforest environments, and specifically in the Amazon rainforest, are rare [15, 16]. A better knowledge of leaf chlorophyll content in the tropical forest is required to contribute to detecting and modeling vegetation stress during drought or pollution events by using satellite data and in this way better understand the potential of photosynthetic capacity and its implications in regional and global carbon cycle and climate models.

Traditional methods for estimating pigment content in vegetation need to be performed in a well-equipped laboratory. They require the extraction of plant pigments from the leaves by applying organic solvents such as dimethyl sulfuoxide (DSMO), methanol, ethanol, acetone, or ether. Depending on the solvent being used, the position of the maximum absorption of plant pigments varies due to the differences in polarity and the loss of pigment-protein interaction [17]. The extracted foliar solution is analyzed by a spectrophotometer in specific absorption wavelength ranges. Finally, absorbance is converted to chlorophyll concentration by applying equations described in the literature [18–21].

Alternative, nondestructive methods for chlorophyll estimation are available from spectral methods for plant pigment estimation. These methods are based on measuring light reflectance and transmittance properties of the vegetation using field spectroradiometers that can be carried in a rucksack, or from spectroradiometers on board of drones, planes, and satellites. They provide indirect estimations of relative pigment content expressed as an index, which needs to be converted to foliar pigment content through often a linear, a polynomial, or an exponential model. During the years, various vegetation indices (VIs) have been developed and applied to remotely sensed satellite images to quantitatively characterize the physiological status of vegetation. VIs are dimensionless measures that indicate relative abundance and activity of green vegetation, including leaf-area-index (LAI), percentage green cover, chlorophyll content, green biomass, and absorbed photosynthetically active radiation (APAR) [22]. VIs are obtained by adding, multiplying, or taking ratios of reflectance in two or more spectral bands of a pixel. These indices are classified into red/NIR ratios, green, red edge, and derivative indices. A useful description of chlorophyll indices can be found in [12, 17] and carotenoid indices [23–25].

This chapter focuses on the analysis of several optical approaches to estimate chlorophyll content in the tropical forest. The study sites were carefully selected across of a forest gradient degradation caused by land uses changes during the last decades. The optical approaches considered are transmittance, reflectance, and radiative transfer models at leave levels; and satellite-derived vegetation indexes at regional level. The objective of this study was to identify suitable methods to detect forest degradation caused by land use changes, deforestation, forest degradation, and pollution in the Amazon rainforest.

2. Alternative methods to measure chlorophyll content

2.1. Chlorophyll meter SPAD-502

Chlorophyll meters based on transmittance have been produced and are available commercially. They offer an inexpensive, easy, rapid, and portable approach for an indirect estimation of chlorophyll content. One of these is the SPAD-502 chlorophyll meter (SPAD-502, Konica-Minolta, Osaka, Japan) which bases its measurements on the light that is transmitted by the leaf in two wavelength regions: the first is located in the red region at 650 nm, which corresponds to the chlorophyll absorption peak unaffected by carotene, and the second is located in the infrared region at 940 nm where chlorophyll absorption is extremely low. The light emitted by the instrument and transmitted by the leaf is measured by the receptor and converted into electrical signals. Finally, a chlorophyll index is calculated by using the ratio of the intensity of the transmitted light [26]. Chlorophyll meters have been used extensively in agriculture to estimate chlorophyll and nitrogen in different species [27–31] and also in forest studies [15, 32–36]. Furthermore, chlorophyll meters have been used in the indirect assessment of foliar nitrogen [29, 30, 37], and carotenoid content [29, 38].

Chlorophyll content estimates in the tropical rainforest are rare. A published generalized homographic model for trees of the Amazon region [15] has been used as standard model to estimate chlorophyll content for more than 700 Amazonian tree species. A comparison of chlorophyll estimation between the homographic model and the second-order polynomial model proposed in this study illustrates good agreement for a wide range of SPAD-502 reading (15–95 units).

The accuracy of the SPAD-502 decreases at high chlorophyll index readings. When applying the proposed second-order polynomial model, caution should be taken for readings higher than 80 where estimation increases markedly compared to other optical methods (reflectance indices and PROSPECT) assessed in this study. Moreover, SPAD index has shown to be a valuable indicator to detect main impacts of land use changes in the tropical forest.

2.2. Reflectance indices

Another spectral method for chlorophyll content estimation is based on reflectance measurements to create pigment indices. Such indices take into account between two and four spectral bands and have shown high accuracy. Despite the literature offers several pigment indices, the majority of them have been tested in just specific plant species or vegetation type. As a result, they have become plant or vegetation specific. Estimations of chlorophyll content based on reflectance indices have been widely used [23–25, 33, 39–42].

Chlorophyll indices are increasingly being used in crops and forest assessments but also in ecology and Earth science. Several calibration models have been described in the literature, most of which, however, have been calibrated and validated in few or closely related plant species with a limited number of samples. Under these conditions, most of the models can only be applied to specific species and environmental conditions [23, 32, 43]. There is no scientific consensus as to whether a universal model can be found that can be applied for species-rich forest stands in different latitudes, phenological stages, and leaf structures [17]. Feret et al. [25] noted this limitation of the spectral indices and proposed new indices for chlorophyll and carotenoid estimation. They were based on a vegetation dataset collected in various ecosystems around the world including a wide variety of plant physiology and leaf structure.

2.3. Radiative transfer models: PROSPECT model

Based on the relationship between reflectance and the biochemical and biophysical properties of the leaves and canopies, models have been created in order to simulate the interaction of the light with the plant leaves through the radiative transfer theory. The leaf optical properties spectra (PROSPECT) model describes radiative transfer within a broadleaf with a plate model [44]. Plate models treat internal leaf structure as sheets or plates and calculate multiple reflections of diffuse radiation between these interfaces [13]. PROSPECT is based on the representation of the leaf as one or several absorbing plates with a rough surface giving rise to isotropic scattering. The model estimates the directional-hemispherical reflectance and transmittance of leaves across the solar spectrum from 400 to 2500 nm [45].

A leaf structure parameter of the model is represented by N, which is the number of compact layers specifying the average number of air/cell wall interfaces within the mesophyll. The leaf biophysical parameters of the model are represented by chlorophyll $a + b$ content (C_{ab}) and equivalent water thickness (C_w). The latest versions of the model include the parameters dry matter content (C_m) and brown pigments content (C_{bp}). Inversion of PROSPECT revealed good agreement between measured and predicted leaf chlorophyll concentrations [13, 45].

2.4. MTCI satellite vegetation index

The medium resolution imaging spectrometer (MERIS) terrestrial chlorophyll index (MTCI) is a standard product derived from MERIS satellite from the European Space Agency (ESA), which provides estimations of chlorophyll content of vegetation (amount of chlorophyll per unit area of ground) at global level. MTCI index is simple to calculate, sensitive to high values of chlorophyll content [46, 47] and estimations are independent to soil and atmospheric conditions, spatial resolution, and illumination and observation geometry [48]. Validation of MTCI index and ground chlorophyll content across a range of crop types and environmental conditions resulted in a strong relationship of $R^2 = 0.8$ and root mean square error (RMSE) = 192 g per MERIS pixel [49]. Moreover, the strong relationship of MTCI and canopy chlorophyll content has been used to estimate gross primary production (GPP) across a range of ecosystems. Boyd et al. [50] applied MTCI index, together with radiation information (photosynthetically active radiation—PAR and fraction of photosynthetically active radiation—fPAR), into models which extended the accuracy of GPP estimated.

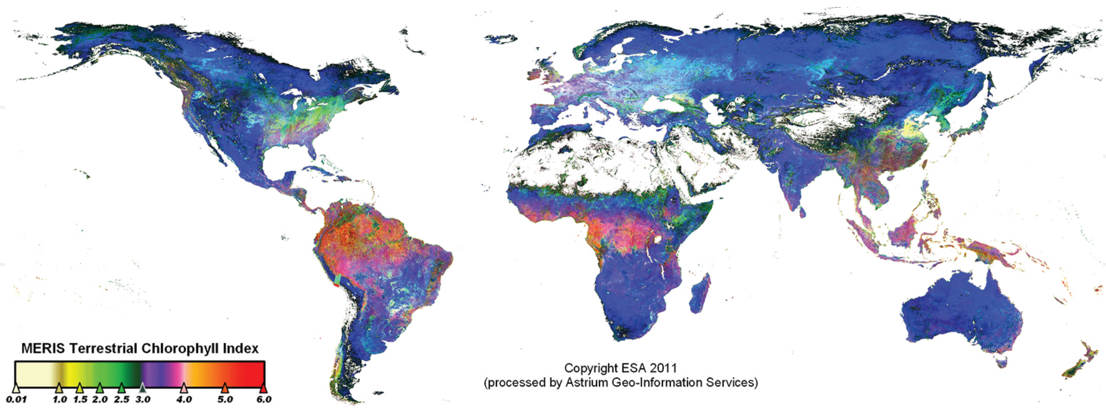

Figure 1. Global coverage of MERIS Terrestrial Chlorophyll Index at 31 May 2011. Processed by Astrium Geo-Information Services. Copyright ESA-2011.

MTCI is computed by the ratio of the difference in reflectance between band 10 and band 9 and the difference in reflectance between band 9 and band 8 of the MERIS standard band setting:

$$MTCI = \frac{R_{\text{Band10}} - R_{\text{Band9}}}{R_{\text{Band9}} - R_{\text{Band8}}} = \frac{R_{753.75} - R_{708.75}}{R_{708.75} - R_{681.25}} \tag{1}$$

where $R_{753.75}$, $R_{708.75}$, and $R_{681.25}$ are the MERIS reflectance at wavelength 753.75, 708.75, and 681.25 nm, respectively.

Figure 1 illustrates the global (Level 3) MERIS terrestrial chlorophyll index (MTCI) estimated at 31 May 2011. Highest MTCI values are located in the tropical forest biomes around the world.

2.5. The red-edge position (REP)

The red-edge position is a unique feature of green plants related to leaf chlorophyll content and to LAI. REP is defined as the inflection point (or sharp change) of the low red reflectance caused by chlorophyll absorption near 680 nm and high infrared reflectance governed by the internal structure of leaves near 750 nm [51]. REP has been used as an indicator of chlorophyll content in vegetation, as increasing chlorophyll content implies an enlargement of the chlorophyll absorption peak: this moves the red-edge to longer wavelengths while a decrease in chlorophyll shifts the red-edge toward shorter wavelengths [12]. However, the REP has been reported not to be an accurate indicator of chlorophyll content in vegetated areas showing high chlorophyll content values because of the asymptotic relationship between REP and chlorophyll content [52, 53].

Several methods have been proposed to estimate REP from spectral data coming from field and satellite sensors. Dawson and Curran [54] developed a three-point Lagrangian interpolation technique, but this method has shown some problems when the reflectance spectrum exhibits more than one maximum in its first derivative [51]. Another method was developed by Guyot and Baret [55], which applies a linear model to the red-NIR slope. This method has been reported to be robust when it was applied to various datasets [11]. A third method identifies the red-edge inflection point as the maximum of a curve fitted to the first derivative of the reflectance spectrum. This method has been closely related to chlorophyll content per unit area at leaf and canopy level [56] and has shown sensitivity to detect vegetation stress by quantifying changes in chlorophyll content [57].

3. Materials and methods

Fieldwork was undertaken from April to Jul 2012 at three sites in the Amazon tropical rainforest of Ecuador (**Figure 1**). The first and second study sites are located in a lowland evergreen secondary forest in Sucumbios province, Tarapoa region (0°11′ S, 76°20′ W). Site 1 has a history of petroleum pollution during the last decades. Mean annual rainfall is 3800 mm and the average annual temperature is 23°C with relative humidity close to 90% [58]. The area is located at 232–238 m above mean sea level. The third study site is a highly diverse lowland evergreen primary forest located in the Orellana province, in the northern section of Yasuní National Park (0°41′ S, 76°24′ W). The area lies 216–248 m above mean sea level and receives an annual average of 3081 mm rainfall with peaks in October and November. Mean monthly temperatures vary from 22°C to 34°C [59]. In this site, the Pontifical Catholic University of Ecuador established and manages permanent forest dynamics plots of 50 hectares where over 150,000 mapped trees ≥1 cm in diameter at breast height (dbh) from over 1100 species have been identified [60].

On one hand, the three study sites are located in the lowland Amazon forest sharing very similar ecological and environmental conditions. On the other hand, the forest in the three sites is substantially different due to the land use changes occurred during the last decades. Site 1 and Site 2 are disturbed forest that was exposed to selective logging, agricultural activities, petroleum industry impacts, and secondary forest regrowth over the last 20 years following diminishing human influence. Site 3 is a pristine primary tropical rainforest with legal protection status where a research project on plant and animal species diversity is currently conducted. Studies consider that the plant species richness in this area is among the highest in the world [61].

3.1. Sampling process

Well-developed branches were carefully selected and collected by using a telescopic pruner, tree-climbing techniques, and canopy towers at different levels of the vertical profile of the forest (**Figure 2**). The collected branches were sealed in large polyethylene bags to maintain their moisture content and stored in ice coolers. The foliar material was transported to a local site, and fully expanded mature leaves with no damage by herbivores or pathogens were selected for analysis. A total of 1134 samples were collected in the three fieldwork sites. The sampling process accounted for three levels of the vertical profile and included a wide range

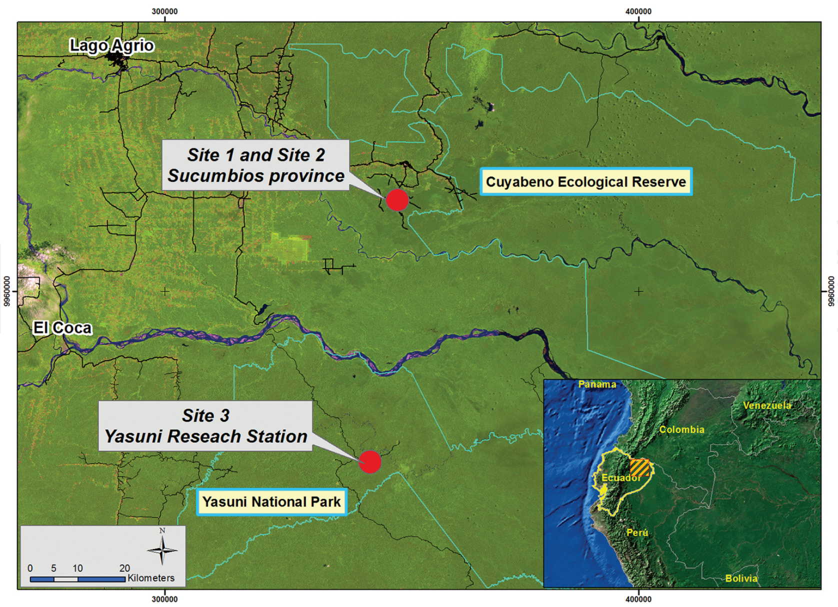

Figure 2. Map of the study area—north-east Amazon region of Ecuador. Site 1 and Site 2 are located in Sucumbios province and Site 3 is located in Orellana province. Background is a Landsat image. Source of zoom-in map: Color shaded relief image, WorldSat International, Inc.

of vegetation heterogeneity related to species distribution, phenological stage, and leaf structure. (Detailed information about the sampled process can be found in Ref. [62].)

3.2. Chlorophyll meter readings

Depending on the size and shape of the leaf, different cork borers of variable size between 2.5 and 8.5 cm diameter were used to clip a leaf disk from the central and widest portion of the leaf blade, avoiding the major veins (**Figure 3**).

Figure 3. Photographs of leaf sampling process. (a) Collecting leaves using the telescopic pruner (b) climbing trees (c) telescopic pruner 9 m long (d) climbing trees techniques and (e) canopy towers in the study area.

All leaf disks were clipped from the midpoint of the leaves since it has been documented that it is the best position from which to take chlorophyll readings [37]. Three readings were taken from each disk using a portable SPAD-502 chlorophyll meter at different positions of each leaf disk, and a mean index value was used in further analysis.

3.3. Spectroradiometer measurements

Reflectance and "trans-flectance" (a term used in this study to describe the measurement of "double" transmittance) were measured for each leaf disk using an ASD FieldSpec Hand-Held-2 spectroradiometer (Analytical Spectral Devices Inc., Boulder, CO, USA). This instrument provides a wavelength range of 325–1075 nm with a resolution of full width at half maximum of 3.5 nm and sampling interval of 1 nm. The spectrometer is attached with a plant probe to an internal 4.05 W halogen light source and a leaf clip that includes rotating head with both white and black reference panels (**Figure 4**).

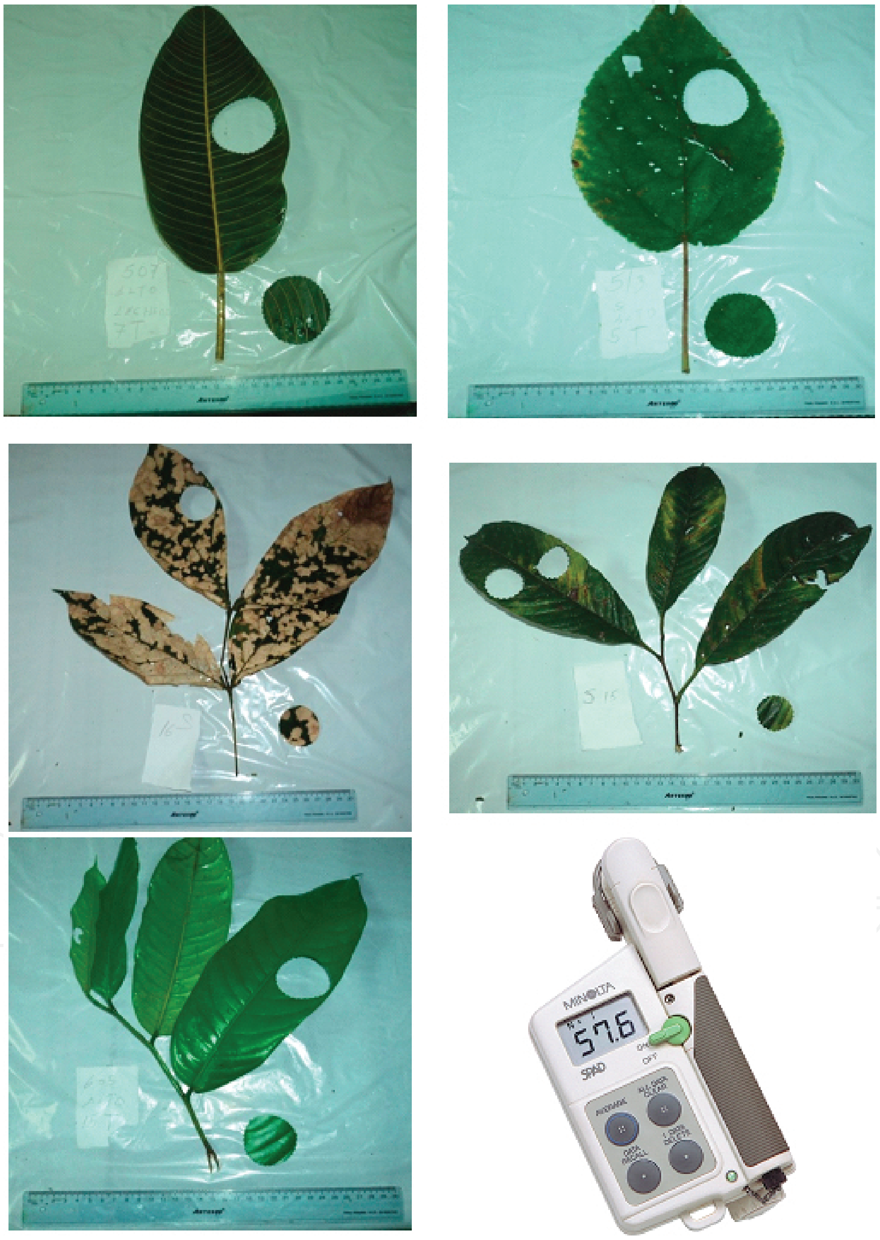

Figure 4. Leaf samples and clipped disks from plants of different species and health status. The last photo shows the SPAD-502 meter.

3.4. Chlorophyll indices based on SPAD-502 readings (transmittance)

Several published calibration models based on SPAD-502 readings were applied in this study. **Table 1** describes seven published polynomial, exponential, or homographic calibration models for chlorophyll content estimation from SPAD-502 chlorophyll meter readings. Selected calibration models cover a heterogeneous range of plants species, plant physiology, phenology, and growing conditions, which is a characteristic of the vegetation in tropical forests. All selected models have shown good agreement with traditional methods applied in a laboratory.

ID	Model	Units	Tested in	Number of samples	SPAD-502 range	Chl range (μm cm^{-2})	R^2
1	Chl = 62.05$e^{(X*0.0408)}$	mg cm^{-2}	6 Amazonian trees species	30–50 leaves per specie	3–80	~0–100	0.79
2	Chl = (117.1*X)/(148.84–X)	μg cm^{-2}	13 Amazonian trees species	391	0–80	0–150	0.89
3	Chl = 2E-05X^2 + 1E-04X + 0.0038	mg cm^{-2}	Lindera melissifolia	145	3.8–47.3	4–50	0.90
4	Chl = 5.52E-04 + 4.04E-04X + 1.25E-05X^2	mg cm^{-2}	Paper birch	100	~0–45	0.4–45.5	0.96
5	Chl = 10.6 + 7.39X + 0.114X^2	μmol m^{-2}	Soybean and maize	na.	0–70	~0–90	0.96
6	Chl = 10($X^{0.265}$)	μmol m^{-2}	Soybean and maize	na.	na.	~0–90	0.94
7	Chl = 10($X^{0.264}$)	μmol m^{-2}	Maize	na.	na.	na.	0.79

na. = Not available.
Source: (1) Ref. [35], (2) Ref. [15], (3) Ref. [31], (4) Ref. [33], (5) Ref. [28], (6) Ref. [28], and (7) Ref. [28].

Table 1. Indices of chlorophyll content estimation (μm cm^{-2}) based on SPAD-502 chlorophyll meter models applied in this study.

3.5. Chlorophyll indices based on reflectance indices

Five reflectance indices for chlorophyll content estimation found in the literature are described in **Table 2**. They considered the visible, red edge, and near infrared ranges. Chlorophyll content was estimated by applying linear or polynomial models for specific plant species when deriving these models. Selection criteria for reflectance indices were based on their ability to estimate chlorophyll content in a wide range of plant species, plant physiology, phenology, and growing conditions, which is a characteristic of the vegetation in tropical forests.

3.6. PROSPECT radiative transfer model

The inversion of the PROSPECT model using leaf reflectance and transmittance was applied in this chapter in order to estimate chlorophyll concentration. Foliar chlorophyll content (C_{ab}) was computed by the inversion process of PROSPECT 5 for the range of 400–1075 nm using reflectance and transmittance in the sampling interval of 1 nm for the 1134 leaf samples. Brown pigments (C_{bp}) and water content (C_w) were neutralized since foliar samples are green vegetation and the spectra does not show water absorption features.

ID	Index	Model	Units	Tested in	Samples	Chl range (μm cm^{-2})	RMSE	R^2
8	$[1/(R_{680\text{-}730})]-[1/(R_{780\text{-}800})]*R_{755\text{-}780}$	Chl = 3.96*X^2 + 23.86*X – 3.31	μg cm^{-2}	Temperate and tropical tree species and crops	1417	0.3–106.7	6.53	na.
9	R_{708}/R_{775}	Chl = 96.8*X^2 – 209.76*X + 115.08	μg cm^{-2}	Temperate and tropical tree species and crops	1417	0.3–106.7	6.6	na.
10	$(R_{780} - R_{712})/(R_{780} + R_{712})$	Chl = 40.65*X^2 + 121.88*X – 0.77	μg cm^{-2}	Temperate and tropical tree species and crops	1417	0.3–106.7	6.25	na.
11	$(R_{750\text{-}800})/(R_{710\text{-}730})$ -1	Chl = 716.32 * X	mg m^{-2}	Maize and soybean	82	~0–100	6.07	0.95
12	$(R_{770\text{-}800})/(R_{720\text{-}730})$ -1	Chl=37.904 + 1353.7X	mg m^{-2}	Maize	2300	1–80.5	3.8	0.94

na. = Not available.
Source: (8) Ref. [25], (9) Ref. [25], (10) Ref. [25], (11) Ref. [40], and (12) Ref. [42].

Table 2. Chlorophyll content indices based on reflectance derived from spectroradiometer data.

3.7. MTCI index

In this study, MTCI was applied to foliar reflectance data collected at leaf level by the following equation:

$$MTCI_{\text{foliar reflectance data}} = \frac{R_{754} - R_{709}}{R_{709} - R_{681}} \tag{2}$$

where R_{754}, $R_{709.75}$, and R_{681} are the foliar reflectance at wavelength 754, 709, and 681 nm, respectively.

3.8. REP: first derivative method

The red-edge inflection point was estimated by the first derivative method:

$$D_{\lambda(i)} = \frac{R_{\lambda(i)} - R_{\lambda(i-1)}}{\Delta\lambda} \tag{3}$$

where $R_{\lambda(i)}$ and $R_{\lambda(i\text{-}1)}$ are reflectance at wavelength i and $(i - 1)$, respectively.

3.9. Vegetation indices from satellite images: MTCI index

USGS EO-1 Hyperion image was that acquired on 15 February 2005. Hyperion data have a spatial resolution of 30 m^2 with each pixel covering the spectral range, 400–2500 nm. A single image is 7.65 km wide (cross-track) by 185 km long (along-track) covering the study sites 1 and 2 (secondary disturbed sites). After atmospheric and radiometric corrections, see more details in [62], MTCI index was derived to assess from space the main impacts of land use changes on chlorophyll content in the tropical forest.

4. Results

4.1. Chlorophyll content based on SPAD indices

Models 1– 7 shown in **Table 3** were applied to the SPAD-502 chlorophyll meter readings from the tropical forest study sites and the descriptive statistics of the estimates are shown in **Table 3**.

Model	Reference	Max.	Min.	Mean	SD
1	[35]	292.83	11.62	67.02	39.70
2	[15]	203.45	13.48	72.16	28.30
3	[31]	191.73	10.06	72.82	30.21
4	[33]	150.27	9.71	62.43	23.21
5	[28]	154.04	13.48	69.46	23.10
6	[28]	194.22	10.31	72.78	29.87
7	[28]	187.56	10.18	70.80	28.82

Table 3. Descriptive statistics of leaf chlorophyll content (μg cm^{-2}) based on seven published SPAD-502 chlorophyll meter models.

Figure 5 illustrates the chlorophyll content estimations for each model, its average values across models, and the confidence interval of 95% for the binned SPAD-502 readings. Estimations for the first six bins (range 15–80 SPAD-502 index) reported similar values. Average values at the higher SPAD index bin (80–95) show increase differences between models.

Figure 5. (a) ASD Hand Held 2 spectrophotometer (b) plant probe + leaf clip.

4.2. Chlorophyll content based on reflectance indices

Reflectance indices and their respective models were applied to the reflectance spectra to the samples collected for this study. The resulting descriptive statistics are shown in **Table 4**. Most of the mean chlorophyll estimations are lower than their counterpart based on SPAD-502 index.

Model	Reference	Max.	Min.	Mean	SD
8	[25]	126.82	1.06	57.92	17.48
9	[25]	78.63	5.05	53.17	11.26
10	[25]	85.80	6.22	54.37	12.29
11	[40]	101.66	5.86	50.05	14.59
12	[42]	136.69	12.51	65.77	18.91

Table 4. Descriptive statistics of chlorophyll concentration (μg cm^{-2}) from the reflectance models based on the spectroradiometer data.

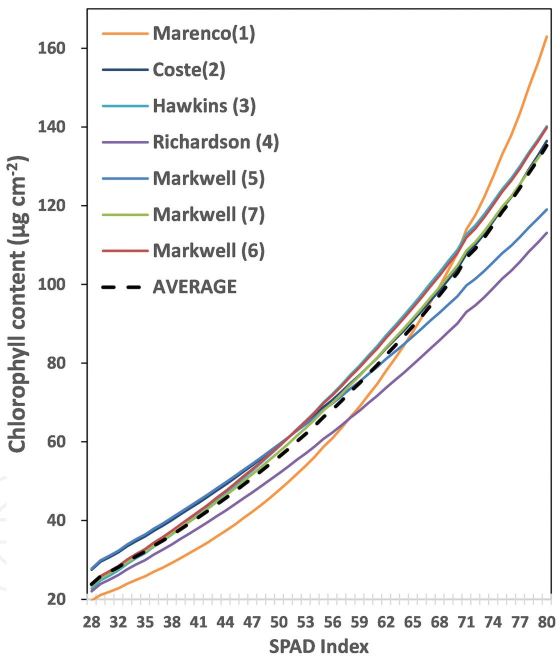

Figure 6. Estimated chlorophyll content for each SPAD-502 calibration model applied to the total samples of our data-set. The black line represents the average value across models and its confidential interval of 95% for the binned SPAD-502 readings.

Figure 6 illustrates the estimations of chlorophyll content for each reflectance model. It includes the average values across models and the 95% confidence interval for the binned SPAD-502 readings. It is interesting to observe that chlorophyll estimations become insensitive for SPAD reading greater than 80.

4.3. Comparison between the three methods for chlorophyll estimation

Figure 7 shows the comparison between average chlorophyll estimations from the three methods used in this study. Estimations until bin 50–60 are relatively similar. Estimation from SPAD then increased exponentially while estimations from reflectance and PROSPECT model are close to each other until bin 70–80, differences then increased since the asymptotic behavior of reflectance models estimations.

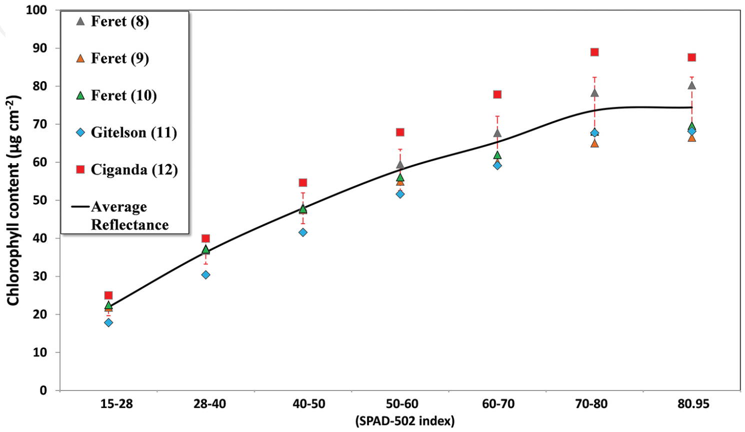

Figure 7. Average chlorophyll content estimates from five reflectance models (errors bars at 1.96 standard deviations) compared to estimated ground truth chlorophyll content based on SPAD-502 chlorophyll meter readings (error bars at 1.96 standard deviations).

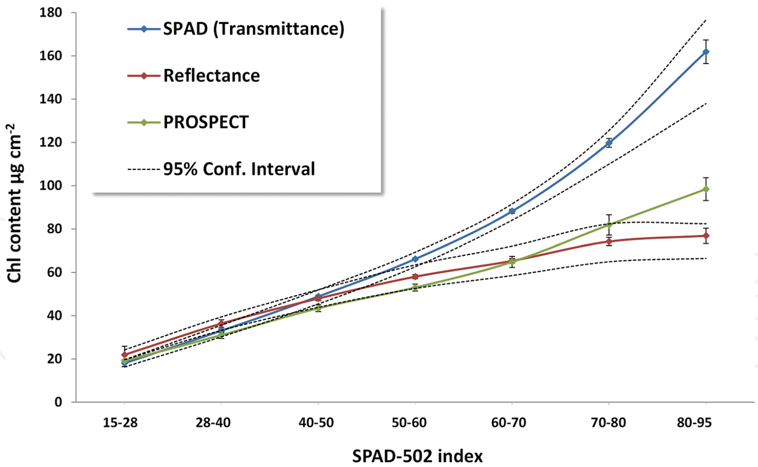

Figure 8. Comparison of average chlorophyll content estimates from the SPAD-502 chlorophyll meter index and the averages of all spectroradiometer-based chlorophyll estimates (error bars at 1.96 standard deviations).

Figure 8 illustrates the comparison of average chlorophyll content estimates from the SPAD-502 chlorophyll meter index and the averages of all spectroradiometer-based chlorophyll estimates. **Figure 9** presents the correspondent boxplots for the three approaches used in this study.

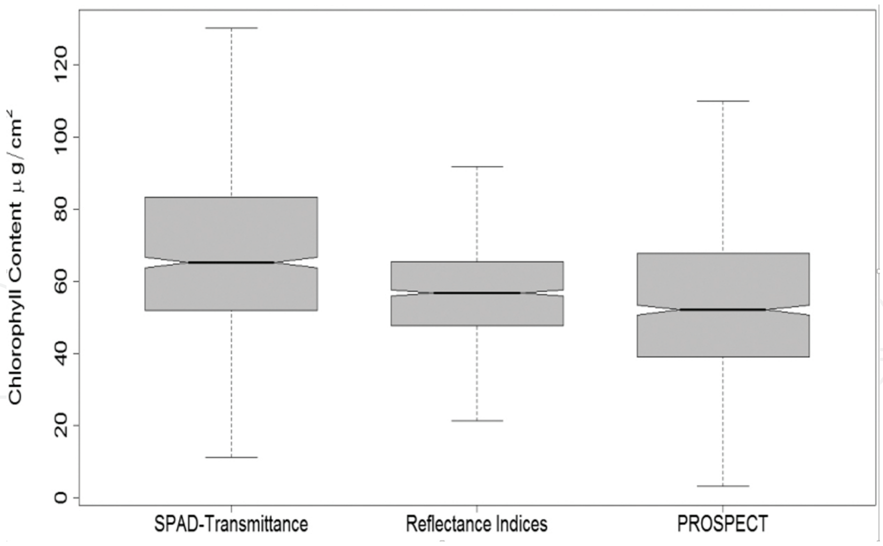

Figure 9. Boxplots of the three estimation of chlorophyll content (outliers not included).

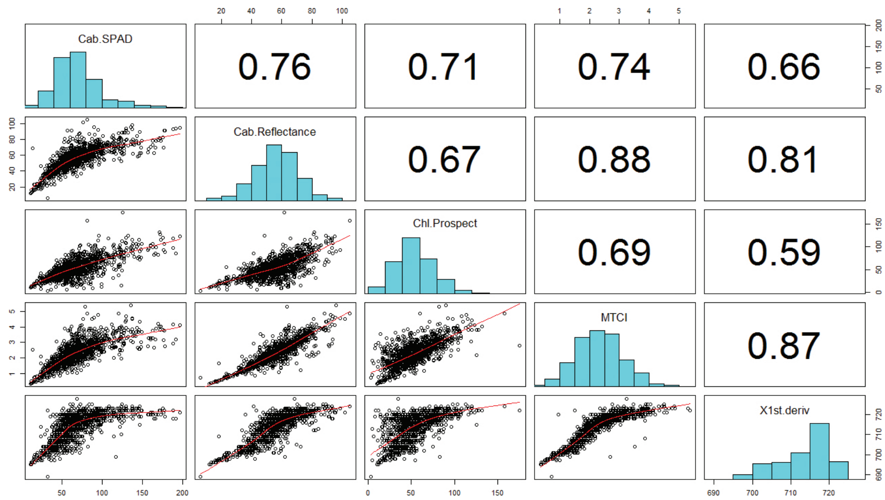

Figure 10. Scatter plots, histograms, and Pearson correlation between three chlorophyll estimations (SPAD, reflectance, and PROSPECT) and MTCI index and REP.

Figure 10 shows the correlations between the three chlorophyll estimations (SPAD-502, reflectance, and PROSPECT) applied in this study. Additionally, correlations with MTCI and REP are presented. Pearson correlation demonstrates a strong correspondence between the three methods calculated at leave level (SPAD-502, reflectance indices, and PROSPECT). Chlorophyll content estimates by the second-order polynomial based on SPAD-502 models and reflectance models agree in 0.76 while SPAD-502 models and PROSPECT agreed in 0.71. The lowest correlation (r = 0.67) is presented by estimations from reflectance models and PROSPECT model despite the fact that both methods are estimated from reflectance measurements. A strong correlation between them was found. MTCI and SPAD-502 correlate in 0.74, MTCI and reflectance models correlate in 0.88, and MTCI and PROSPECT correlate in

0.69. Correlation coefficients between REP and SPAD-502 model, reflectance models, PROSPECT, and MTCI are 0.66, 0.81, 0.59, and 0.87, respectively.

Figure 11 shows the estimations of leaf chlorophyll content based on SPAD index, MTCI and Ratio of derivatives. For the first two methods, chlorophyll content in the oil spill is significantly lower compared to the non-polluted sites.

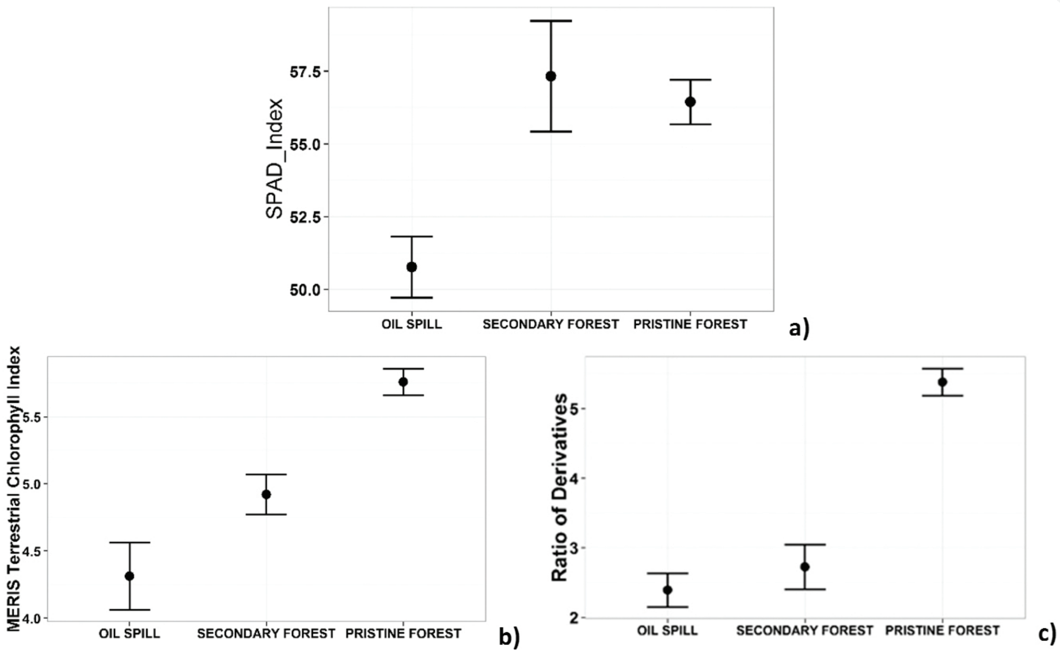

Figure 11. (a) SPAD chlorophyll index for the three study sites; (b) MERIS terrestrial chlorophyll index and (c) REP red-edge position-first derivatives for the three study sites.

4.4. Chlorophyll content evaluation

SPAD 502 chlorophyll content index and REP index were estimated for the three study sites. The results from **Figure 10(a)** and **(c)** shows that chlorophyll content was significantly lower (99.9%) at the secondary forest affected by pollution (Site 1) which allow us to conclude that forest degradation at local level can be detected using a portable chlorophyll content instrument. On the other hand, MTCI index derived from the satellite image also shows significantly lower values in the Site 1 **(Figure 10b)**, which confirm that chlorophyll content is a suitable indicator of land uses changes, and it can be applied at regional level to detect forest degradation caused by land use changes in the tropical forest.

MTCI index at regional level was computed using the Hyperion satellite images of the area corresponding to Site 1 and Site 2. **Figure 12** illustrates the results. Lower levels of chlorophyll (less than four) are found around the petroleum facilities and routes. On the other hand, higher levels of chlorophyll content (more than four) were found in areas still covered by the secondary forest.

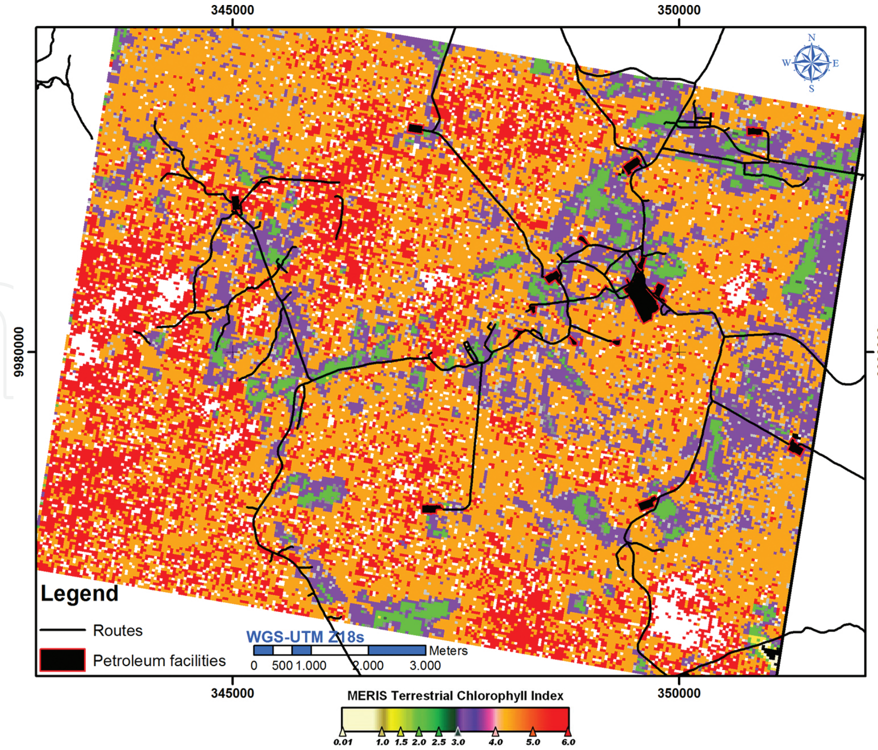

Figure 12. MTCI index computed from the Hyperion Satellite images of the study area of Site 1 and Site 2.

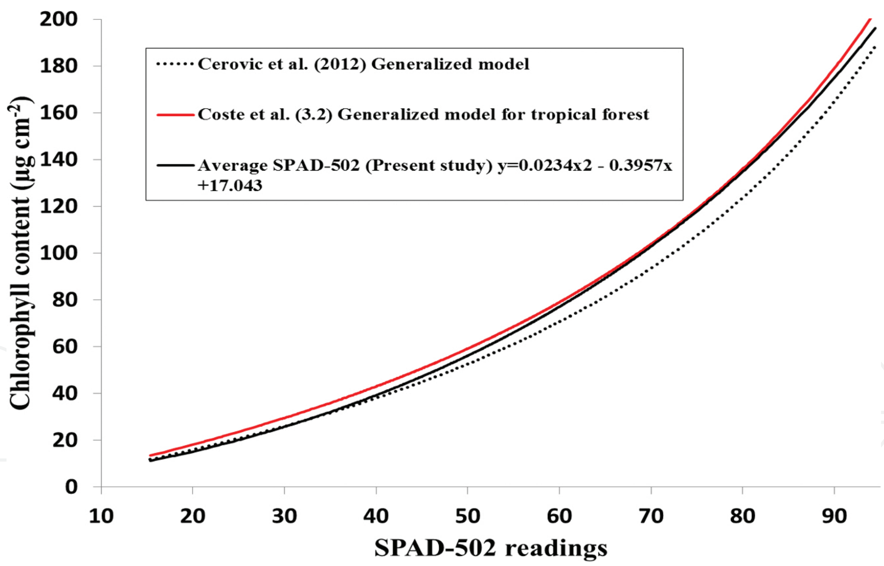

Figure 13. Comparison of three generalized models derived from SPAD-502 readings. The second-order polynomial model proposed in this study (black line), the homographic model proposed by Cerovic et al. [36] (dotted line), and the homographic model proposed by Coste et al. (2012) for trees from the Amazon forest.

Based on the results of the seven SPAD-502 published calibration models we compute their average in order to obtain a general model for chlorophyll content estimation which accomplish for a wide range of vegetation species and physiological stage. The resulting general model is a second order polynomial in a range of 15 to 95 SPAD index readings. This general model is proposed as ground truth chlorophyll which is assessed by comparing it to a reference published generalized model based on SPAD-502 readings and traditional methods in a laboratory. The first reference model is a homographic model proposed by Cerovic et al. (2012) and computed from seven (polynomial, exponential and homographic) models applied to a variety of plant species. The second model is the generalised homographic model for tropical trees proposed by Coste et al. (2010) which was discussed before as Model 2 in **Table 1**. **Figure 13** illustrates the comparison of the three models.

5. Discussion

Five methods for the estimation of chlorophyll content were applied to the collection of over 1100 leaf samples from the Ecuadorian Amazon rainforest, which represents a wide range of vegetation species growing in a disturbed and a pristine lowland rainforest. The first method is an optical method based on transmittance from the SPAD-502 chlorophyll meter index, the second method, also optical, is based on reflectance measurements collected by a spectroradiometer, and the third method is based on radiative transfer approach using the inversion process of the PROSPECT model. The other two methods are based on vegetation indices derived from satellite images.

For the first method, seven models that account for a wide range of vegetation species, phenological stage, and leaf structure showed close estimations between them until 80 SPAD-502 index (**Table 3** and **Figure 5**). At higher indices the differences increase. This can be explained by the fact that the calibration models considered a maximum SPAD-502 range of 80 units, meanwhile our database register readings beyond this range until 95 units. The best accuracy claimed by the instrument reaches its maxima until 50 units; therefore, higher values may be less accurate.

Based on the results of the seven SPAD-502 published calibration models, we compute their average in order to obtain a general model for chlorophyll content estimation which accomplish for a wide range of vegetation species and physiological stage. The resulting general model is a second-order polynomial in a range of 15–95 SPAD index readings. This general model is proposed as ground truth chlorophyll which is assessed by comparing it to a reference published generalized model based on SPAD-502 readings and traditional methods in a laboratory. The first reference model is a homographic model proposed by Cerovic et al. [36] and computed from seven (polynomial, exponential, and homographic) models applied to a variety of plant species. The second model is the generalized homographic model for tropical trees proposed by Coste et al. [15], which was discussed before as Model 2. **Figure 11** illustrates the comparison of the three models.

The proposed second-order polynomial model has the same concave shape and very close chlorophyll estimations along the range 15-95 SPAD-502 readings than the two homographic models. Homographic models have the generalized equation proposed by Cerovic et al. [36] and claims to be probably more accurate and certainly more rapid and portable than wet methods when used in crop plants. The model proposed by Coste et al. [15] was developed for the tropical forest from the Amazon region and has been a reference model for estimating chlorophyll content based on SPAD-502 readings.

Indeed, published SPAD-502 models applied to tropical rainforest vegetation are rare. A literature search by the authors only found two models (Model 1 and Model 2) developed for several species of the Amazon forest. Both experiments with tropical trees of the Amazon exhibited higher SPAD-502 readings which are comparable with our dataset. Those models account for a wide range of species, leaf structure, and phenology, and claim good accuracy for chlorophyll content estimation in multispecies forest stands. The homographic model proposed by Coste et al. [15] (Model 2) has been used to estimate chlorophyll content in a study that considered 1084 trees from 758 species across a broad environment gradient of 13 sites (seasonal flooded, clay terra firma, and white-sand forest) at opposite ends of Amazonia in Guiana and Peru [63]. The study relies on chlorophyll estimations based on the SPAD-502 model without considering traditional methods in a laboratory which prove the ability of a rapid and portable method of chlorophyll content in remote areas where analysis in a laboratory is not available.

Based on the comparison to published homographic models for multispecies, it is derived that the second-order polynomial calibration model offers a good approximation of chlorophyll content in tropical forest species. This is because of its close performance compared to the models proposed by Cerovic et al. [36] and Coste et al. [15] (**Figure 10**), and its homographic nature takes into consideration the reduced performance of chlorophyll meters at high chlorophyll contents. Indeed a homographic nature of SPAD-502 model has been applied to a wide range of tropical species from the Amazonia [63].

Estimations from the second method based on five reflectance models illustrate good agreements along all range of SPAD-bins (15–95 units). **Table 4** and **Figure 6** illustrate the results of these methods showing a saturation curve at the higher SPAD bind (80–95).

The observed maximum values of chlorophyll estimation from SPAD-502 (**Table 3**) are considerably higher than maximum values from reflectance indices (**Table 4**), which reflect the exponential increase of SPAD-502 models after 80 SPAD-502 units and the asymptotic nature of reflectance indices after this range. Differences between average estimations are less distinctive.

The first two methods are compared with the third method which is based on the inversion process of the PROSPECT model. **Figure 7** illustrates that the mean values are close to each other until 50–60, and after that the estimations based on SPAD-502 models increase faster than the other two methods. The method based on reflectance models and the PROSPECT model show close mean values until bin 70–80. Analysis of variance (ANOVA) and pairwise comparison between the three methods shown in **Table 5** indicate significant difference between the methods. Results from the lower SPAD-502 bin reported no differences between the methods.

	ANOVA	Pairwise comparisons between chlorophyll estimation methods (Holm adjustment method)		
	p-value	SPAD vs. reflectance	SPAD vs. PROSPECT	Reflectance vs. PROSPECT
All dataset	***	***	***	*
<28	ns	ns	ns	ns
28–40	***	**	.	***
40–50	***	ns	***	***
50–60	***	***	***	***
60–70	***	***	***	ns
70–80	***	***	***	**
80>	***	***	***	***

ns, nonsignificant.
***Strongly significant (0.1%) or lowest significant (10%).
**Highly significant (1%).
*Significant (5%).

Table 5. ANOVA and pairwise comparison between the three chlorophyll methods for chlorophyll estimation based on the binned SPAD-502 index.

Table 5 shows ANOVA and pairwise comparison between the three chlorophyll methods for chlorophyll estimation based on the binned SPAD-502 index.

Figure 10 presented that the chlorophyll estimations at leave level (SPAD-502, reflectance indices, and PROSPECT model) and estimations at regional level (satellite images) applied in this study show strong correlations between them. This finding demonstrates that a combination of field-based methods at leaf level with remote sensing methods at regional level may provide a good opportunity to evaluate forest health caused by land use changes. As it was stated in the introduction, forest degradation and its related changes in ecosystem services have not been fully assessed using remote sensing techniques, especially in high diverse tropical forest. The estimations of MTCI index in Site 1 and Site 2 shown in **Figure 12** have demonstrated lower levels of chlorophyll content caused by land use changes, specifically due the influence of petroleum facilities cause forest degradation. Therefore, in those areas accurate estimations of photosynthetic activity of forested areas are needed to quantify forest degradation and evaluate environmental services provided by flora in the tropical forest.

6. Conclusion

Three optical methods for estimation of chlorophyll content at leaf level were applied to the collection of over 1100 leaf samples collected in the Ecuadorian Amazon rainforest, which represents a wide range of vegetation species growing in a disturbed and a pristine lowland rainforest. The first method is based on transmittance from the SPAD-502 chlorophyll meter index, the second method is based on reflectance measurements collected by a spectroradiometer, and the third method estimates chlorophyll content from the radiative transfer PROSPECT model. For the first method, seven models that account for a wide range of

http://dx.doi.org/10.5772/65493

vegetation species showed similar average leaf chlorophyll contents until 80 units of SPAD-502. An average of the results of these models was computed and used as ground truth from where a generalized second-order polynomial model was created. For the second method, five chlorophyll indices based on reflectance measurements provided similar chlorophyll content estimations for all SPAD range (15–95 units). The third method estimates chlorophyll content based on the inversion process of the PROSPECT model.

Comparison between the three methods shows that estimations until bin 50–60 are relatively similar, and estimations from SPAD increased exponentially. Estimations from reflectance and the PROSPECT model are close to each other until bin 70–80, after that differences increased since the asymptotic behavior of reflectance models estimations. A strong coefficient of correlations between the proposed generalized model and reflectance and PROSPECT approaches result in 0.76 and 0.71, respectively. Comparisons with MTCI and REP indicate correlations of 0.74 and 0.66, respectively.

The results of this study show that the relatively lightweight handheld field spectroradiometer can be used at field level to estimate leaf chlorophyll content in remote tropical rainforest ecosystems that are difficult to access. They provide a rapid and portable method for such remote areas where traditional chemical extraction methods for chlorophyll estimation are not viable. A general second-order polynomial calibration model for chlorophyll content estimation which accounts for a wide range of plant species, phenological stage, and leaf structure based on spectral measures offers an alternative approach for chlorophyll estimation. At a regional level, vegetation indices derived from satellite images are an efficient approach to detect chlorophyll content differences in vegetation exposed to main impacts of land use changes in the Amazon forest. These methods can be applied to regional scale to monitor the effects environmental services provided by the tropical forest and to detect forest degradation caused by land use changes.

Author details

Paul Arellano[1,2,3*], Kevin Tansey[3] and Heiko Balzter[3,4]

*Address all correspondence to: parellano@yachaytech.edu.ec; pa134@le.ac.uk

1 Yachay Tech University, School of Geological Sciences & Engineering, San Miguel de Urcuquí, Imbabura, Ecuador

2 Centre of Earth Observation, Yachay Tech University, San Miguel de Urcuquí, Hacienda, Imbabura, Ecuador

3 University of Leicester, Department of Geography, Centre of Landscape and Climate Research, Leicester, UK

4 National Centre for Earth Observation, University of Leicester, Leicester, UK

References

[1] FAO, "Global forest resources assessment," FAO Forestry Paper, vol. 140, pp. 281–286, 2001.

[2] R. Roy, B. Saugier and H. Mooney, Terrestrial Global Productivity, in San Diego, 2001.

[3] B. Groombridge and M. Jenkins, World Atlas of Biodiversity, University of California Press, 2003.

[4] Y. Malhi, J. T. Roberts, R. A. Betts, T. J. Killeen, W. Li and C. A. Nobre, "Climate change, deforestation, and the fate of the Amazon," Science, vol. 319, pp. 169–172, 2008.

[5] E. A. Davidson, A. C. De Araüjo, P. Artaxo, J. K. Balch, I. F. Brown, M. M. C. Bustamante, M. T. Coe, R. S. Defries, M. Keller, M. Longo, J. W. Munger, W. Schroeder, B. S. Soares-Filho, C. M. Souza Jr. and S. C. Wofsy, "The Amazon basin in transition," Nature, vol. 481, pp. 321–328, 2012.

[6] O. L. Phillips, L. E. O. C. Aragão, S. L. Lewis, J. B. Fisher, J. Lloyd, G. López-González, Y. Malhi, A. Monteagudo, J. Peacock, C. A. Quesada, G. Van Der Heijden, S. Almeida, I. Amaral, L. Arroyo, G. Aymard, T. R. Baker, O. Bánki, L. Blanc, D. Bonal, P. Brando, J. Chave, Á. C. A. De Oliveira, N. D. Cardozo, C. I. Czimczik, T. R. Feldpausch, M. A. Freitas, E. Gloor, N. Higuchi, E. Jiménez, G. Lloyd, P. Meir, C. Mendoza, A. Morel, D. A. Neill, D. Nepstad, S. Patiño, M. C. Peñuela, A. Prieto, F. Ramírez, M. Schwarz, J. Silva, M. Silveira, A. S. Thomas, H. T. Steege, J. Stropp, R. Vásquez, P. Zelazowski, E. A. Dávila, S. Andelman, A. Andrade, K. Chao, T. Erwin, A. Di Fiore, E. C. Honorio, H. Keeling, T. J. Killeen, W. F. Laurance, A. P. Cruz, N. C. A. Pitman, P. N. Vargas, H. Ramírez-Angulo, A. Rudas, R. Salamão, N. Silva, J. Terborgh and A. Torres-Lezama, "Drought sensitivity of the Amazon rainforest," Science, vol. 323, pp. 1344–1347, 2009.

[7] R. A. Houghton, K. T. Lawrence, J. L. Hackler and S. Brown, "The spatial distribution of forest biomass in the Brazilian Amazon: A comparison of estimates," Global Change Biology, vol. 7, pp. 731–746, 2001.

[8] UNFCCC, "Reducing emissions from deforestation in developing countries approaches to stimulate actions," Decision 2/CP, 13, 2007.

[9] R. A. Houghton, "Carbon emissions and the drivers of deforestation and forest degradation in the tropics," Current Opinion in Environmental Sustainability, vol. 4, pp. 597–603, 2012.

[10] A. Hoscilo, "Fire regime, vegetation dynamics and land cover change in tropical peatland, Indonesia," 2009.

[11] J. G. P. W. Clevers, S. M. De Jong, G. F. Epema, F. D. Van der Meer, W. H. Bakker, A. K. Skidmore and K. H. Scholte, "Derivation of the red edge index using the MERIS standard band setting," International Journal of Remote Sensing, vol. 23, pp. 3169–3184, 2002.

[12] H. G. Jones and R. A. Vaughan, Eds., Remote Sensing of Vegetation. Principles, Techniques and Applications, New York: Oxford University Press, 2010.

[13] L. Kumar, K. Schmidt and S. Dury, "Imaging spectrometry and vegetation science," in Imaging Spectrometry. Basic Principles and Prospective Applications, 4th ed., F. van del Meer and S. de Jong, Eds., Dordrecht, The Netherlands: Springer, 2006, pp. 111–155.

[14] K. L. Smith, J. J. Colls and M. D. Steven, "A facility to investigate effects of elevated soil gas concentration on vegetation," Water, Air, & Soil Pollution, vol. 161, pp. 75–96, 2005.

[15] S. Coste, C. Baraloto, C. Leroy, É. Marcon, A. Renaud, A. D. Richardson, J. Roggy, H. Schimann, J. Uddling and B. Hérault, "Assessing foliar chlorophyll contents with the SPAD-502 chlorophyll meter: A calibration test with thirteen tree species of tropical rainforest in French Guiana," Annals of Forest Science, vol. 67, pp. 607p1–607p5, 2010.

[16] K. F. Cao and E. W. Booth, "Leaf anatomical structure and photosynthetic induction for seedlings of five dipterocarp species under contrasting light conditions in a Bornean heath forest," Journal of Tropical Ecology, vol. 17, pp. 163–175, 2001.

[17] S. L. Ustin, A. A. Gitelson, S. Jacquemoud, M. Schaepman, G. P. Asner, J. A. Gamon and P. Zarco-Tejada, "Retrieval of foliar information about plant pigment systems from high resolution spectroscopy," Remote Sensing of Environment, vol. 113, pp. S67–S77, 2009.

[18] D. I. Arnon, "Copper enzymes in isolated chloroplasts. Polyphenoloxidase in Beta Vulgaris," Plant Physiology. American Society of Plant Biologists, vol. 24, pp. 1–15, 1949.

[19] J. D. Hiscox and G. F. Israelstam, "A method for the extraction of chlorophyll from leaf tissue without maceration," Canadian Journal of Botany, vol. 57, pp. 1332–1334, 1979.

[20] H. K. Lichtenthaler, "[34] Chlorophylls and carotenoids: Pigments of photosynthetic biomembranes," Methods in Enzymology, vol. 148, pp. 350–382, 1987.

[21] R. J. Porra, W. A. Thompson and P. E. Kriedemann, "Determination of accurate extinction coefficients and simultaneous equations for assaying chlorophylls a and b extracted with four different solvents: Verification of the concentration of chlorophyll standards by atomic absorption spectroscopy," BBA – Bioenergetics, vol. 975, pp. 384–394, 1989.

[22] J. R. Jensen, Remote Sensing of the Environment: An Earth Resource Perspective, USA: Pearson Education, Inc., 2007.

[23] A. A. Gitelson, Y. Gritz and M. N. Merzlyak, "Relationships between leaf chlorophyll content and spectral reflectance and algorithms for non-destructive chlorophyll

assessment in higher plant leaves," Journal of Plant Physiology, vol. 160, pp. 271–282, 2003.

[24] A. A. Gitelson, G. P. Keydan and M. N. Merzlyak, "Three-band model for noninvasive estimation of chlorophyll, carotenoids, and anthocyanin contents in higher plant leaves," Geophysical Research Letters, vol. 33, pp. L11402, 2006.

[25] J. Féret, C. François, A. Gitelson, G. P. Asner, K. M. Barry, C. Panigada, A. D. Richardson and S. Jacquemoud, "Optimizing spectral indices and chemometric analysis of leaf chemical properties using radiative transfer modeling," Remote Sensing of Environment, vol. 115, pp. 2742–2750, 2011.

[26] Konica Minolta, "Chlorophyll meter SPAD-502Plus. Instruction manual," 2009.

[27] O. A. Monje and B. Bugbee, "Inherent limitations of nondestructive chlorophyll meters: A comparison of two types of meters," HortScience, vol. 27, pp. 69–71, 1992.

[28] J. Marwell, J. Osterman and J. Mitchell, "Calibration of the Minolta SPAD-502 leaf chlorophyll meter," Photosynthesis Research, vol. 46, pp. 467–472, 1995.

[29] A. Torres-Netto, E. Campostrini, J. Gonçalves de Oliveira and O. Yamanishi, "Portable chlorophyll meter for the quantification of photosynthetic pigments, nitrogen and the possible use for assessment of the photochemical process in Carica papaya L.," Brazilian Journal of Plant Physiology, vol. 14, pp. 203–210, 2002.

[30] A. Torres-Netto, E. Campostrini, J. Gonçalves de Oliveira and R. Bressan-Smith, "Photosynthetic pigments, nitrogen, chlorophyll a fluorescence and SPAD-502 readings in coffee leaves," Scientia Horticulturae, vol. 104, pp. 199–209, 2005.

[31] T. S. Hawkins, E. S. Gardiner and G. S. Comer, "Modeling the relationship between extractable chlorophyll and SPAD-502 readings for endangered plant species research," Journal for Nature Conservation, vol. 17, pp. 125–129, 2009.

[32] A. D. Richardson, "Changes in foliar spectral reflectance and chlorophyll fluorescence of four temperate species following branch cutting," Tree Physiology, vol. 22, pp. 499–506, 2002.

[33] A. D. Richardson, S. P. Duigan and G. P. Berlyn, "An evaluation of noninvasive methods to estimate foliar chlorophyll content," New Phytologist, vol. 153, pp. 185–194, 2002.

[34] K. L. Castro-Esau, G. A. Sánchez-Azofeifa, B. Rivard, S. J. Wright and M. Quesada, "Variability in leaf optical properties of mesoamerican trees and the potential for species classification," American Journal of Botany, vol. 93, pp. 517–530, 2006.

[35] R. A. Marenco, S. A. Antezana-Vera and H. C. S. Nascimento, "Relationship between specific leaf area, leaf thickness, leaf water content and SPAD-502 readings in six Amazonian tree species," Photosynthetica, vol. 47, pp. 184–190, 2009.

[36] Z. G. Cerovic, G. Masdoumier, N. B. Ghozlen and G. Latouche, "A new optical leaf-clip meter for simultaneous non-destructive assessment of leaf chlorophyll and epidermal flavonoids," Physiologia Plantarum, vol. 146, pp. 251–260, 2012.

[37] B. O. Hoel, "Use of a hand-held chlorophyll meter in winter wheat: Evaluation of different measuring positions on the leaves," Acta Agriculturae Scandinavica – Section B Soil and Plant Science, vol. 48, pp. 222–228, 1998.

[38] L. Poorter, R. Kwant, R. Hernández, E. Medina and M. J. A. Werger, "Leaf optical properties in Venezuelan cloud forest trees," Tree Physiology, vol. 20, pp. 519–526, 2000.

[39] B. Datt, "Remote sensing of water content in Eucalyptus leaves," Australian Journal of Botany, vol. 47, pp. 909–923, 1999.

[40] A. A. Gitelson, A. Viña, V. Ciganda, D. C. Rundquist and T. J. Arkebauer, "Remote estimation of canopy chlorophyll content in crops," Geophysical Research Letters, vol. 32, pp. 1–4, 2005.

[41] A. Gitelson, O. Chivkunova and M. N. Merzlyak, "Nondestructive estimation of anthocyanins and chlorophylls in anthocyanic leaves," American Journal of Botany, vol. 96, pp. 1861–1868, 2009.

[42] V. Ciganda, A. Gitelson and J. Schepers, "Non-destructive determination of maize leaf and canopy chlorophyll content," Journal of Plant Physiology, vol. 166, pp. 157–167, 2009.

[43] D. A. Sims and J. A. Gamon, "Relationships between leaf pigment content and spectral reflectance across a wide range of species, leaf structures and developmental stages," Remote Sensing of Environment, vol. 81, pp. 337–354, 2002.

[44] S. Jacquemoud and F. Baret, "PROSPECT: A model of leaf optical properties spectra," Remote Sensing of Environment, vol. 34, pp. 75–91, 1990.

[45] S. Jacquemoud, "PROSPECT SAIL models: A review of use for vegetation characterization," Remote Sensing of Environment, vol. 113, pp. S56–S66, 2009.

[46] J. Dash and P. J. Curran, "The MERIS terrestrial chlorophyll index," International Journal of Remote Sensing, vol. 25, pp. 5403–5413, 2004.

[47] M. L. España-Boquera, R. Cárdenas-Navarro, L. López-Pérez, V. Castellanos-Morales and P. Lobit, "Estimating the nitrogen concentration of strawberry plants from its spectral response," Communications in Soil Science and Plant Analysis, vol. 37, pp. 2447–2459, 2006.

[48] P. J. Curran and J. Dash, Algorithm Theoretical Basis Document ATBD 2.2: Chlorophyll Index, Southampton, UK: University of Southampton, 2005.

[49] J. Dash, P. J. Curran, M. J. Tallis, G. M. Llewellyn, G. Taylor and P. Snoeij, "Validating the MERIS Terrestrial Chlorophyll Index (MTCI) with ground chlorophyll content data

at MERIS spatial resolution," International Journal of Remote Sensing, vol. 31, pp. 5513–5532, 2010.

[50] D. S. Boyd, S. Almond, J. Dash, P. J. Curran, R. A. Hill and G. M. Foody, "Evaluation of envisat MERIS terrestrial chlorophyll index-based models for the estimation of terrestrial gross primary productivity," IEEE Geoscience and Remote Sensing Letters, vol. 9, pp. 457–461, 2012.

[51] J. P. G. W. Clevers and R. Jongschaap, "Imaging spectrometry for agricultural applications," in Imaging Spectrometry, F. van der Meer and S. M. de Jong, Eds., The Netherlands: Springer, 2006, pp. 157–199.

[52] R. A. Jago, M. E. J. Cutler and P. J. Curran, "Estimating canopy chlorophyll concentration from field and airborne spectra," Remote Sensing of Environment, vol. 68, pp. 217–224, 1999.

[53] R. Munden, P. J. Curran and J. A. Catt, "The relationship between red edge and chlorophyll concentration in the Broadbalk winter wheat experiment at Rothamsted," International Journal of Remote Sensing, vol. 15, pp. 705–709, 1994.

[54] T. P. Dawson and P. J. Curran, "A new technique for interpolating the reflectance red edge position," International Journal of Remote Sensing, vol. 19, pp. 2133–2139, 1998.

[55] G. Guyot, F. Baret and D. J. Major, "High spectral resolution: Determination of spectral shifts between the red and the near infrared," International Archives of Photogrammetry and Remote Sensing, vol. 11, pp. 740–760, 1988.

[56] G. A. Blackburn, "Quantifying chlorophylls and caroteniods at leaf and canopy scales: An evaluation of some hyperspectral approaches," Remote Sensing of Environment, vol. 66, pp. 273–285, 1998.

[57] K. L. Smith, M. D. Steven and J. J. Colls, "Use of hyperspectral derivative ratios in the red-edge region to identify plant stress responses to gas leaks," Remote Sensing of Environment, vol. 92, pp. 207–217, 2004.

[58] L. J. Fitton, "Helminthiasis and culture change among the cofán of ecuador," American Journal of Human Biology, vol. 12, pp. 465–477, 2000.

[59] R. Valencia, "Yasuni forest dinamic plot, ecuador," in Tropical Forest Diversity and Dynamism: Findings from a Large-Scale Plot Network, E. Losos, J. Leigh and E. Giles, Eds., Chicago: University of Chicago Press, 2004, pp. 609–628.

[60] R. Valencia, R. B. Foster, G. V. Richard-Condit, J. C. Svenning, C. Hernández, K. Romoleroux, E. Losos, E. Magards and H. Balslev, "Tree species distributions and local habitat variation in the Amazon: Large forest plot in eastern Ecuador," Journal of Ecology, vol. 92, pp. 214–229, 2004.

[61] L. Tedersoo, A. Sadam, M. Zambrano, R. Valencia and M. Bahram, "Low diversity and high host preference of ectomycorrhizal fungi in Western Amazonia, a neotropical biodiversity hotspot," ISME Journal, vol. 4, pp. 465–471, 2010.

[62] P. Arellano, K. Tansey, H. Balzter and D. S. Boyd, "Detecting the effects of hydrocarbon pollution in the Amazon forest using hyperspectral satellite images," Environmental Pollution, vol. 205, pp. 225–239, 2015.

[63] C. Fortunel, P. V. A. Fine and C. Baraloto, "Leaf, stem and root tissue strategies across 758 neotropical tree species," Functional Ecology, vol. 26, pp. 1153–1161, 2012.